applied sciences

MDPI

Article

Analysis of the Progressive Collapse Resistance Mechanism of an RC Frame Structure with an L-Shaped Plane

Yifei Dai and Lei Qin *

Department of Civil Engineering, Hubei University of Technology, Wuhan 430068, China
* Correspondence: 102110929@hbut.edu.cn; Tel.: +86-178-3710-5254

Abstract: In order to improve the progressive collapse resistance of an RC frame structure with an L-shaped plane under local component failure, X-tension reinforcement and steel trusses are applied to the progressive collapse resistance design. In this paper, the finite element software MIDAS Gen v2.1 is used to establish the RC frame structure with 6-story X-type tension strengthening and the RC frame structure with a steel truss at the top. Nonlinear dynamic analysis and a comparison of the two structures after local structural failure are carried out. The results show that both X-tension reinforcement and steel trusses can improve the integrity of the RC frame structure with an L-shaped plane and reduce the risk of progressive collapse in the event of single-column failure, but the steel trusses have the best effect. After component failure, adding a steel truss to the top layer can transfer the load above the failure column to other columns and reduce some beam resistance, providing a more effective alternative load transfer path for the structure.

Keywords: progressive collapse; numerical simulation; steel truss; nonlinear dynamic analysis

check for updates

Citation: Dai, Y.; Qin, L. Analysis of the Progressive Collapse Resistance Mechanism of an RC Frame Structure with an L-Shaped Plane. *Appl. Sci.* **2023**, *13*, 7216. https://doi.org/10.3390/app13127216

Academic Editors: Chiara Bedon, Flavio Stochino and Filipe Amarante dos Santos

Received: 22 May 2023
Revised: 7 June 2023
Accepted: 13 June 2023
Published: 16 June 2023

1. Introduction

Extreme events (i.e., terrorist attacks, vehicle impacts, explosions, etc.) often cause local damage to building structures and pose a serious threat when one or more vertical load-bearing components fail, leading to the progressive collapse of the entire structure or a large part of it. As it is difficult to predict the probability of occurrence and the magnitude of extreme events, it is neither practical nor possible to design a structure against them through the traditional methods for conventional loads. To avoid progressive collapses, alternative load paths must be available for the load supported by the damaged column to be transferred to neighboring elements. Most current studies on progressive collapse focus on regular RC frame structures [1–3], and relatively few studies focus on irregular RC frame structures. However, with the increase in building height and complexity and the wide application of irregular building structures, progress collapse accidents often occur [4,5]. Under the action of accidental load, the asymmetric distribution of mass and stiffness of an irregular structure is more likely to cause the failure of this structure than of a regular structure.

The alternate load path method (APM), a significant design approach to reduce progressive collapse, has been mentioned by a number of design codes including GSA [6] and DoD [7]. The APM allows local failure to occur when subjected to an extreme load, but seeks to provide an alternate load path so that the initial damage can be contained and major collapse can be averted. For designing new buildings or checking the capacity of a structure, the technique can be employed. Adding a new structural member to provide additional alternate load paths is a classic approach for strengthening structural systems against progressive collapse. For example, Bandyopadhyay et al. [8] studied the progressive collapse of both unbraced and braced semi-rigid jointed steel frames in order to evaluate the contribution of bracing to improving the progressive collapse resistance. Yu et al. [9] proposed a steel bracing design method based on incremental dynamic analysis (IDA) in order to explore the influence of steel bracing on RC frame resistance to progressive collapse. Ke et al. [10], in order to improve the progressive collapse resistance of general RC frame structures under local component failure, applied X-tension reinforcement to the progressive collapse resistance design. Qiu et al. [11] proposed a strengthening method to improve the collapse resistance of RC frame structures by installing steel cables of a preset length at the bottom of the beams. The test and analysis results showed that the ultimate resistance of the modified substructure is 90–255% higher than that of the unmodified substructure when two steel cables with diameters of 10 or 14 mm are used as beam and column components. Freddi et al. [12] added a truss steel system (i.e., "roof truss") to the roof layer of the building, aiming to define an alternative load path, which was investigated as a retrofit solution. Zahrai et al. [13] proposed a method of cap trusses and steel struts to resist the progressive collapse of intermediate RC frame structures. It was found that the axial forces in the removed columns were transferred to adjacent columns by alternative paths using cap trusses to prevent partial or integral failure, or to delay the occurrence of progressive collapse.

Because collapse tests cost a lot of money and the test process is complicated, numerical simulation is still the main method to study the progressive collapse resistance of a structure. Kiakojouri et al. [14] analyzed in detail the influence of finite element modeling and analysis techniques (including the solution process, mesh size, element type, column-removal time, damping, strain rate and output-related problems) on the nonlinear dynamic column-removal response of steel frame structures. Stephen et al. [15] used different numerical methods to simulate the sudden removal of columns in frame structures, and discussed the influence of rising time on the structural response. At present, the three most commonly used dynamic analysis methods for collapse simulation are the instantaneous stiffness degradation method, the instantaneous loading method and the initial condition method [16]. The instantaneous stiffness degradation method simulates the failure of components to be removed by reducing the stiffness of the components to be removed to 0. The instantaneous loading method firstly removes a part of the component, and then applies instantaneous reaction force on the remaining structure to simulate the failure of the component. The initial condition method obtains the static internal forces of the components to be removed before the failure of the structure, applies reaction forces after the removal of the components in the remaining structure, and applies constant and live loads to the overall structure. After the remaining structure reaches a static balance, the reaction force of the components to be removed is suddenly removed to simulate the failure of the components.

At present, studies that have used the nonlinear analysis of RC frame structures with L-shaped planes against progressive collapse are relatively few. In this paper, the initial condition method is combined with the nonlinear implicit dynamics method to build a model in MIDAS Gen, and the progressive collapse nonlinear dynamic analysis is carried out for RC frame structures with the addition of X-type tensions and a steel truss at the top. The internal force and displacement of the two structures are studied under the failure condition of a single column, and the data are compared and analyzed.

2. Structural Modeling

2.1. Irregular Structure

A regular structure means that the structure has symmetry and uniformity, its component size does not change much, the facade is continuous, the vertical load is continuous and uniform, and the load transfer path does not change significantly in the horizontal plane and vertical plane.

The opposite of a regular structure is an irregular structure. It is indicated in the United States UBC-97 specification that a structure is planar irregular when its projection in two directions exceeds the length portion of the concave edge and is greater than 15% of the plane dimensions of the direction considered by the structure. The force of irregular structures under accidental loads is complicated, and thus the force transmission path is not clear, which can easily cause damage to the weak parts of the structure and lead to the progressive collapse and breakage of local structures, or even of the whole structure [17].

According to the Chinese Standard for Seismic Design of Buildings (GB 50011-2010), if the concave size is greater than 30% of the total size of the corresponding projection direction, the structure is an irregular plane structure. The types of irregular buildings vary, and their dynamic response under unexpected loads is uncertain, which usually needs to be analyzed by nonlinear dynamic analysis. In order to avoid the progressive collapse of such buildings, continuity, redundancy and durability are required [18].

2.2. Project Overview

In this study, a 3-D full-scale finite element model was used to evaluate progressive collapse. All models were designed using the commercial multi-story building analysis program MIDAS Gen. To make sure that the structures in this study are exactly the same as conventional constructs, the structure sections were designed using PKPM software V4.1. The structural model studied in this paper is an irregular L-shaped plane structure, as shown in Figure 1a.

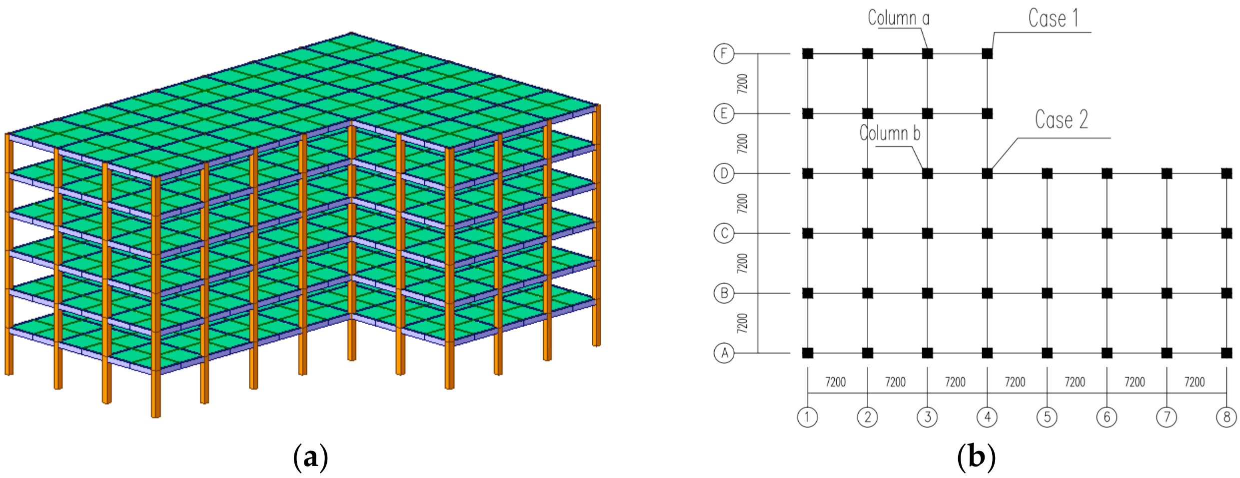

Figure 1. Schematic diagram of irregular frame structure: (**a**) structural elevation diagram; (**b**) floor plan and locations of damage cases (A–F, 1–8 represents the number of the central axis in the plane. Case1 and Case2 are the positions of the failure columns in the plane. Columns a and b represent adjacent columns of the failed column).

The model uses PKPM to build a 6-story-frame office building, as shown in Figure 1b, whose plane structure is L-shaped, with main beams and secondary beams arranged at intervals. The longitudinal and transverse spans are 7.2 m, the height of the first floor is 5.10 m, and the other floors are 4.2 m. The reinforcement and beam-column cross-section are selected in accordance with China's Concrete Structure Design Code (GB 50010-2010) [19], where the main beam cross-section size is 300 mm $\times$ 600 mm, the secondary beam is arranged between the two main beams and the secondary beam cross-section is 250 mm $\times$ 450 mm. The first-floor column cross-section is 650 $\times$ 650 mm, and the standard floor column cross-section is 650 mm $\times$ 650 mm. The live load of the floor and roof slab is 2.0 KN/m^2, the constant load is 5.0 KN/m^2, the floor beam load is 7.5 KN/m, the ground roughness category is B, the modified basic wind pressure is 0.4 KN/m^2, the seismic category is C, the seismic grouping is Group I and the damping ratio of the structure is 0.05. The intensity of protection is 6 degrees. The thickness of the protective layer of beams is 25 mm and that of columns is 30 mm. The reinforcement of the simulated failed first-floor columns is shown in Figure 2a. Column F4 represents the column where axis F intersects axis 4, and D4 represents the column where axis D intersects axis 4. The reinforcement of the main beam adjacent to the failed column is shown in Figure 2b. See Table 1 for reinforcement information.

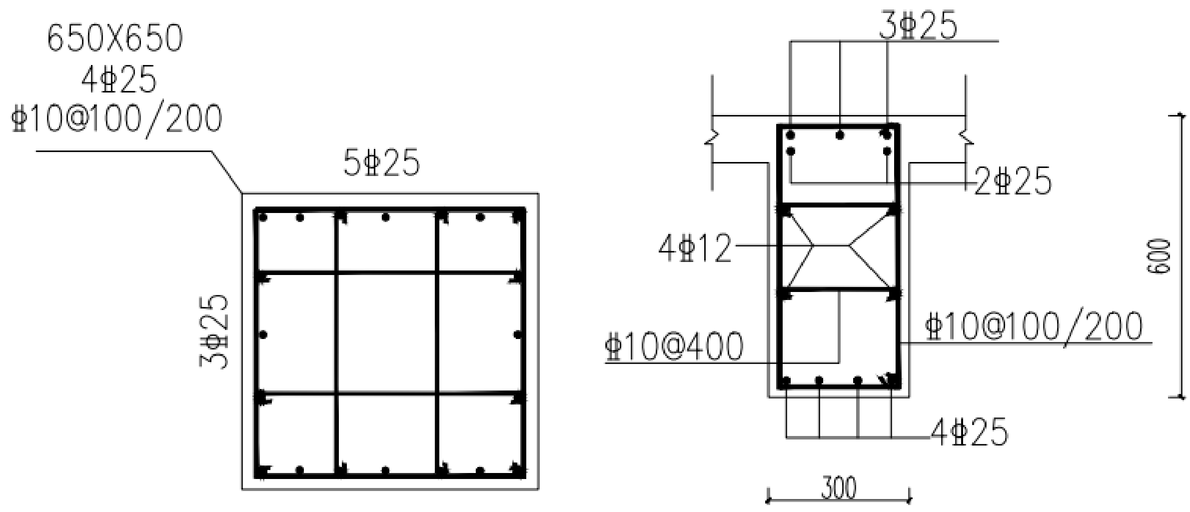

(**a**) (**b**)

Figure 2. Reinforcement figure: (**a**) reinforcement diagram of the first-floor column with simulated failure; (**b**) reinforcement diagram of the main beam adjacent to the failed column.

Table 1. Reinforcement information.

Floor	Main Beam Sectional Dimension (mm)	Secondary Beam Sectional Dimension (mm)	Column Sectional Dimension (mm)	Concrete Intensity	Strength Grade of Beam Column Longitudinal Bar	Stirrup Strength Grade
1	300 × 600	250 × 450	650 × 650	C30	HRB400	HRB400
2–6	300 × 600	250 × 450	600 × 600	C30	HRB400	HRB400

2.3. Type of Reinforcement

The resistance of irregular building structures to progressive collapse is not due to prevention with or the strengthening of individual components, but rather the prevention of possible collapse of the whole building structure is needed, and the integrity of the structure should be considered; thus, when designing the resistance of irregular building structures to progressive collapse, the effective connection of whole structural components should be ensured, and only in this way can the redundancy of the whole structure be increased and its ability to resist progressive collapse be improved [20]. In this paper, the finite element software MIDAS Gen was used to model two strengthening types of irregular building structures. The beam element was used to simulate the beam column, and the elastic floor was used to simulate the floor with equal stiffness. In the model, the boundary was simplified as the fixed constraint of the concrete column at the bottom. Concrete was simulated with a solid unit, and linear reduction unit C3D8R was selected for analysis. The steel bar is simulated by a truss element, specifically T3D2.

Model 1 adds steel trusses to the roof. MIDAS Gen was used to establish the frame structure model and steel truss model and combined the models with the combined data file command in the finite element software, as shown in Figure 3a. The force transfer diagram of the steel truss is shown in Figure 3b. In this model, C30 is used for the frame structure, and Q345 is used for the roof truss system, where its outer diameter is 160 mm, the wall thickness is 120 mm for a hollow round-section steel pipe and its cross-section area is 5579 mm^2. Table 2 shows the amount of steel used in the steel truss in Model 1.

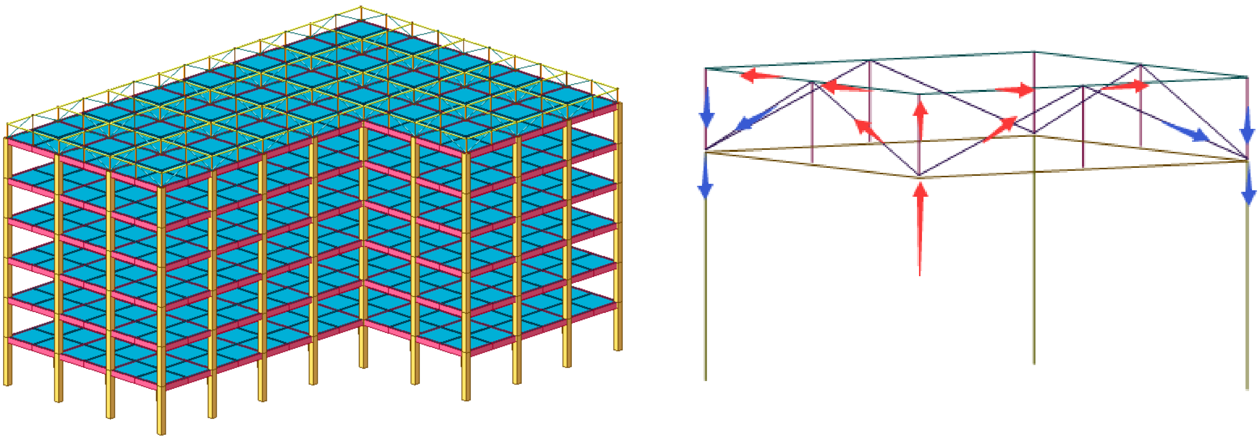

(**a**) (**b**)

Figure 3. Model 1: three-dimensional diagram (**a**); force transfer diagram of steel truss (The red arrow represents the incoming force of the steel truss; The blue arrows represent the force coming out of the steel truss.) (**b**).

Table 2. The amount of steel used in the Model 1 steel truss.

Bar	Length (m)	Amount	Whole Length (m)
Upper chord	3.6	132	475.2
Straight flank rod	1.5	106	159
Diagonal flank rod	3.9	132	514.8

Model 2 is modeled in the same way as Model 1. In Model 2, X tension reinforcement is added to the periphery of the original structure. The diameter of steel cable used for X strengthening is 14 mm and the material is HRB400, as shown in Figure 4a. After the failure of the columns of the structure, the internal forces of the structure will be redistributed. The beams above the failed columns and the surrounding columns will share the internal forces of the failed columns, as shown in Figure 4b. The material properties of rebar are shown in Table 3.

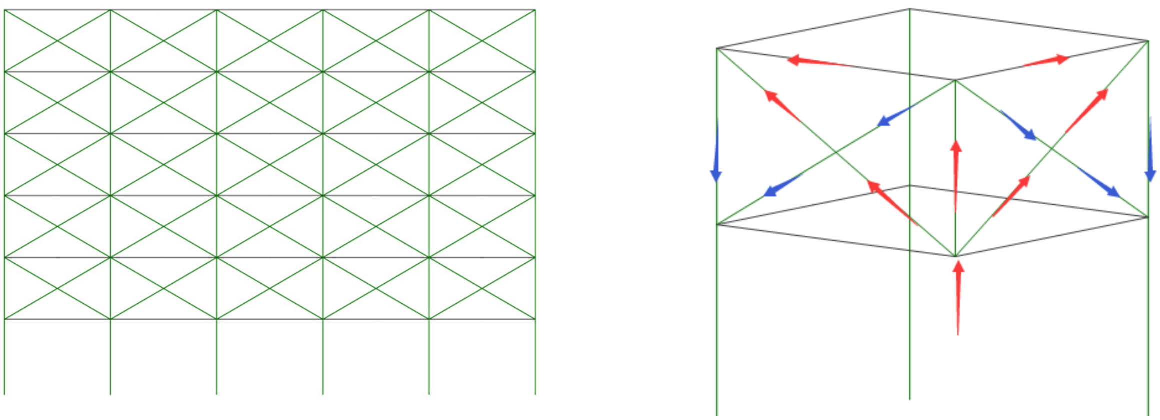

(**a**) (**b**)

Figure 4. X-tension-strengthening frame diagram (**a**); X-tension-strengthening force transfer diagram (The red arrow represents the incoming force of the X-tension-strengthening; The blue arrow represents the force coming out of the X-tension-strengthening) (**b**).

Table 3. Material properties of reinforcing steel bars.

Type	Density (kg/m^3)	Elastic Modulus, E_S (GPa)	Poisson Ration	Yield Strength, fy (MPa)
Q345	7850	210	0.3	345
HRB400	7850	200	0.3	400

3. Theoretical Analysis

3.1. Material Constitutive Analysis

3.1.1. Constitutive Model of Concrete

In this paper, the damage plastic model (CDP model) [21,22] was adopted as a representative for concrete, as it can effectively simulate concrete. The CDP model is mainly used to simulate concrete under monotonic, cyclic and dynamic loads under low confining pressures. The tensile and compressive elastic–plastic and damage models of concrete under uniaxial stress tests are shown in Figure 5. In the figure, d_t represents the tensile damage factor. σ_{t0} is the extreme tensile stress. d_c stands for the compression damage factor, E_0 is the initial elastic modulus of concrete, σ_c is the inelastic stress in compression, $\varepsilon_c{}^{in}$ is the inelastic compressive strain, $\varepsilon_{0c}{}^{in}$ is the elastic compressive strain at the initial stiffness, $\varepsilon_t{}^{pl}$ is the tensile plastic strain, and $\varepsilon_c{}^{pl}$ is the compressive plastic strain.

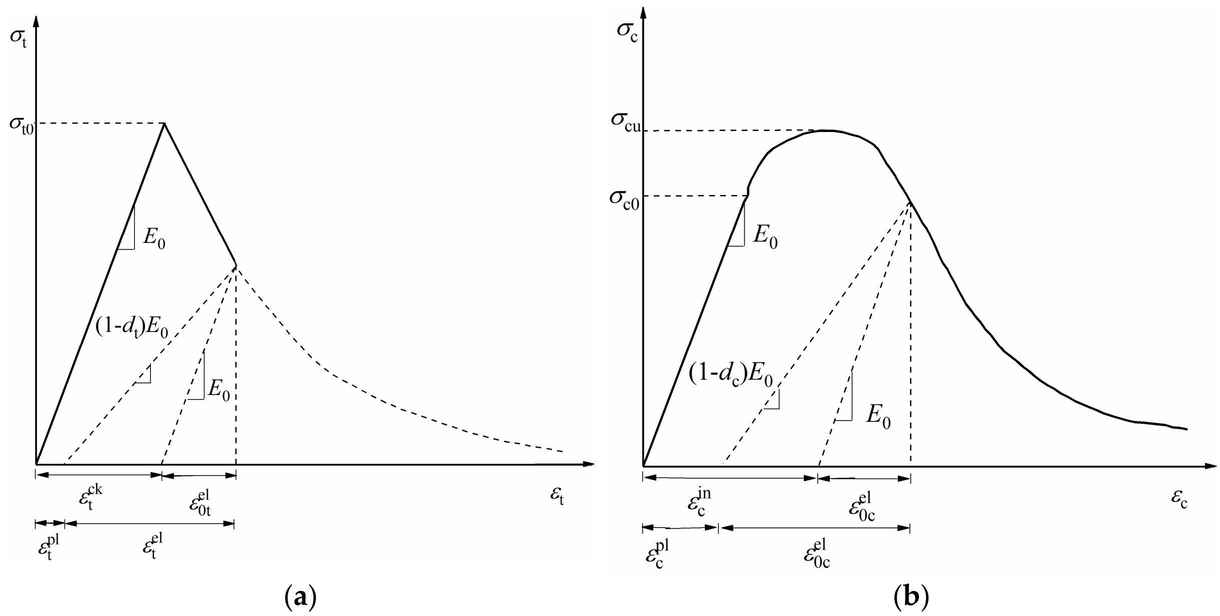

Figure 5. Stress–strain relationship of plastic models of tensile and compressive damage of concrete: (**a**) tensile damage; (**b**) compression impairment.

3.1.2. Constitutive Model of Reinforcement

For the *HRB400* steel bar material, the design value of the steel bar yield strength f_y = 360 N/mm^2, the standard value f_{yk} = 400 N/mm^2, and the elastic modulus of the steel bar E_s = 2 × 105 N/mm^2. In the process of software modeling, the ideal elastic–plastic double-fold model without a yield point is selected according to the stress–strain curve of reinforcement under monotonic loading in the specification [19]. The model does not take into account the fracture of steel bars, which is consistent with the fact that there is no fracture in the steel bars during the test. This model has good applicability in reflecting the yield and strengthening stages of ordinary reinforcement, and its reinforcement constitutive model is shown in Figure 6. E_P = 2.06 × 105 N/mm^2 is the elastic modulus of the steel bar in the ideal elastic–plastic bifold model without a yield point. E_t = 0.01 EP is the elastic modulus of the strengthening stage.

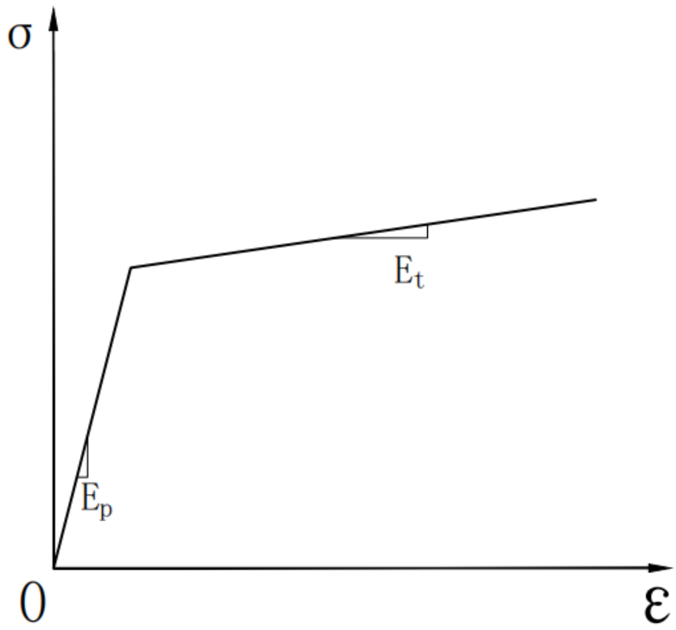

Figure 6. Bilinear isotropic hardening constitutive model.

3.2. Nonlinear Dynamic Analysis

The method of nonlinear dynamic analysis is the initial condition method. The initial condition method obtains the internal forces of the components to be removed under a static force before the failure of the structure, applies the reaction force after the removal of the components in the remaining structure, and applies the constant and live load in the overall structure. When the residual structure reaches static equilibrium, the reaction force of the component to be removed is suddenly removed to simulate the failure of the component [23].

First, the load is applied to the original structure. The load combination is as follows:

$$1.2DL + 0.5LL \quad (1)$$

where DL is the constant load and LL is the live load. The internal force of the original structure under the above load is calculated, and the unbalanced force at the end of the failure column in each working condition is obtained.

Then, the simulated failure column in the original structure is removed. At the same time, the corresponding unbalanced force is applied to the node at the upper end of the simulated failure column to make the structure equivalent to the original structure. In the new model, the constant load and live load of the structure were loaded from t_0 to t_1 according to Figure 7a, and the unbalanced force was loaded according to Figure 7b. The failure of a single column was simulated and nonlinear dynamic analysis was carried out. A stability period (t_1 to t_2) of 1.5 s was taken to ensure the initial equilibrium condition before removing the column. The column-removal time (t_2 to t_3) was considered to be less than one-tenth of the period of vertical motion as per the GSA guidelines, and it was taken as 0.001 s for all of the scenarios [2]. P is the magnitude of the force while $\boldsymbol{t}$ is time.

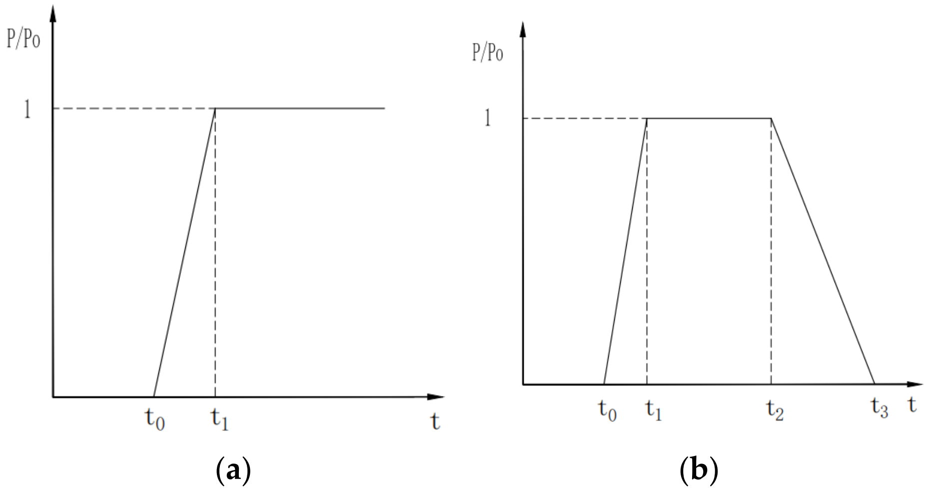

Figure 7. Load function: (**a**) Loading diagram of constant load and live load; (**b**) loading diagram of unbalanced force.

3.3. Model Verification

In this paper, MIDAS Gen was used to simulate a two-story concrete frame collapse experiment that was conducted by the progressive collapse research team of building structures from Chang'an University [24].

The stress nephogram obtained from the test failure diagram and numerical simulation is shown in Figure 8. As can be seen from Figure 8a, the distribution of cracks in the floor shows an arc-shaped crack with the failure column located at the center of the circle. It can be seen from Figure 8b that the stress level of the concrete is high at the bottom of the failure column and the adjacent beam ends, and it is believed that a plastic hinge appears in these parts. On the whole, the experimental phenomenon is in good agreement with the numerical simulation results.

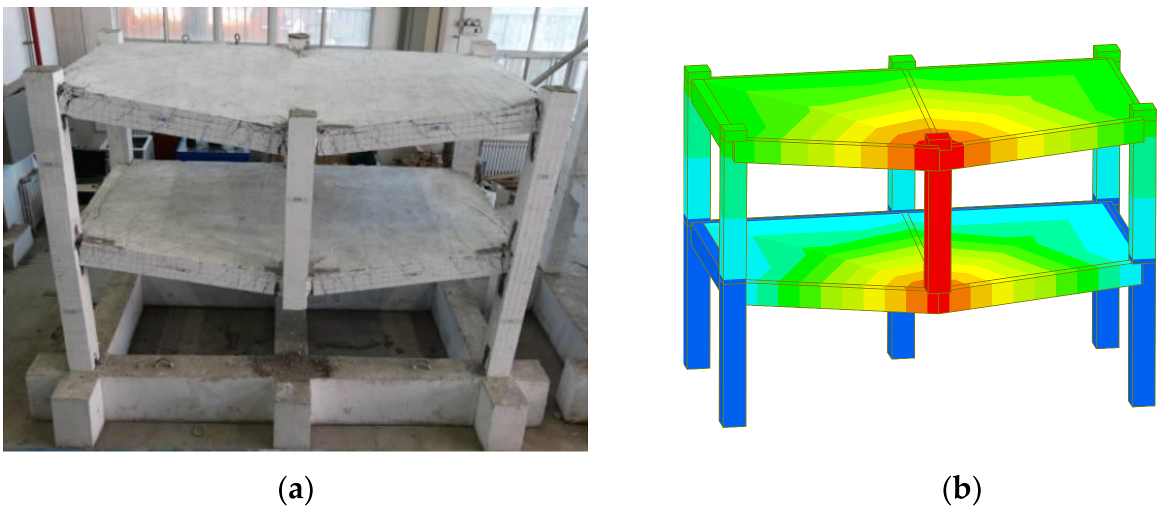

Figure 8. Model test failure diagram (**a**); numerical simulation diagram (**b**).

The simulation value obtained with the loading method by the simulation research team was compared with the experimental data, as shown in Figure 9. By comparing the experimental data with the simulated data, the curve fitting degree is good and the error is within a reasonable range, which indicates the feasibility of the finite element modeling method and parameter selection.

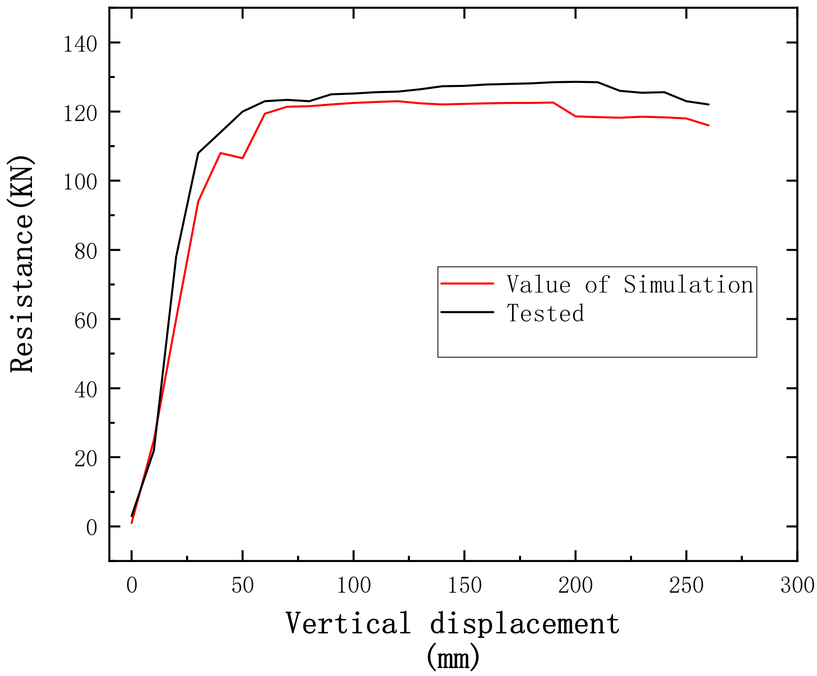

Figure 9. Top resistance–displacement curve of failure column.

4. Discussion

The resistance of the structure to progressive collapse can be reflected by monitoring the vertical displacement curve of the upper surface of the failure column and the internal forces of the adjacent members. According to the United States DoD2005 code, the progressive collapse failure criterion of the structure is defined as the structural collapse that occurs when the relative vertical displacement at both ends of the beam exceeds 1/5 of the net span [7].

In the planar irregular structure, according to the relevant provisions of GSA2003, the influence of the failure of the bottom column that is located at the concave corner of the planar irregular structure should be investigated [6]. According to relevant studies, the failure of the column at the outer convex corner can easily cause the progressive collapse of the structure [23]. Therefore, the test simulation was carried out by removing the column at the outer convex corner on the first floor and the column at the concave corner on the first floor.

4.1. Removal of the Convex-Corner Column

Figure 10 shows the structure displacement nephogram of Models 1 and 2 at 5 s after the first-layer F4 column is removed. Figure 11 shows the vertical displacement time-history curve of the nodes above the failure column after the first-layer F4 column is removed. As can be seen from the figure, the vertical displacement in the original irregular structure increased significantly before 0.75 s, and gradually stabilized to 96.6 mm after 2.6 s. If the value is much smaller than the failure criterion of progressive collapse of the structure, the structure model does not collapse. In Model 1, after the steel truss is added to the roof, the vertical displacement increases rapidly before 0.8 s, then slows down, and gradually becomes stable at 53.4 mm after 2.1 s. Compared with the original structure, the vertical displacement is reduced by 44.7%. In Model 2, the vertical displacement increased rapidly before 0.92 s after the addition of the X-type tensile-strengthening structure, and gradually stabilized to 76.3 mm after 1.3 s. Compared with the original structure, the vertical displacement is reduced by 21.1%.

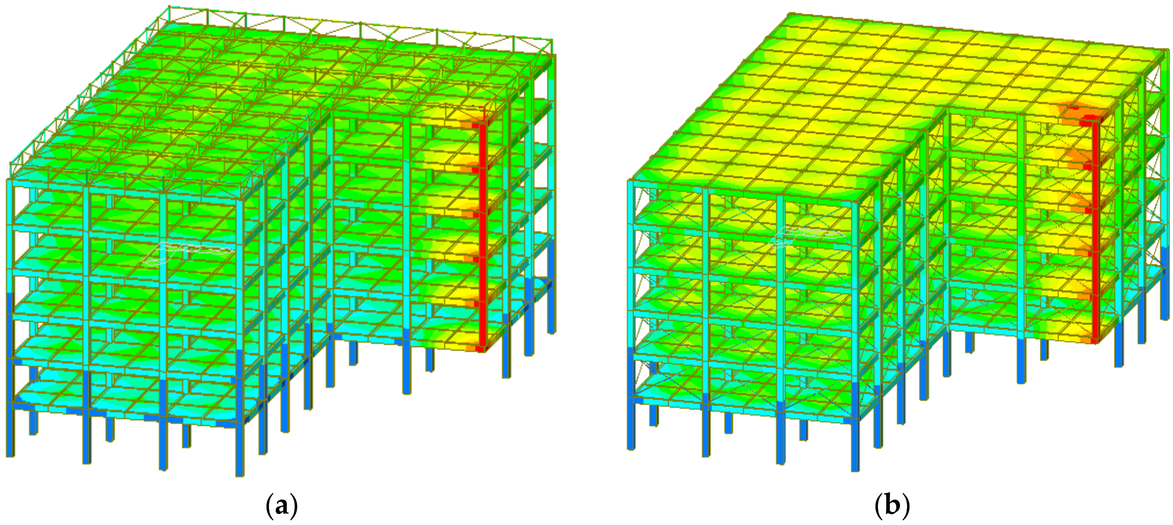

Figure 10. Displacement nephogram of structure at convex-corner column-removal condition: (**a**) Model 1 with roof-added steel trusses; (**b**) X-tension reinforcement is added to Model 2 structure.

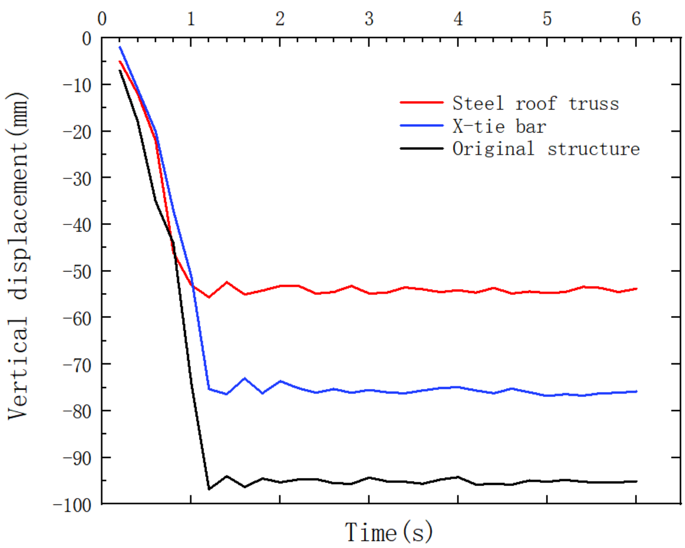

Figure 11. Time-history diagram of removal displacement of columns at convex corners of each model.

The vertical displacement development trend of each model is consistent with the original model. By comparing the vertical displacement above the failure column with the convex-corner column in the balance, we can see that adding a steel truss to the roof can reduce the vertical displacement caused by the failure of the corner column more effectively; additionally, adding X-tie strengthening to the structure can also reduce the vertical displacement caused by the failure of the corner column, but the effect is not as significant as the former.

Figures 12 and 13 show internal force diagrams of the F-axis 5 s after the first-layer F4 column is removed. In the modified Model 1, the square column above the failure column is subjected to axial tension, and the maximum bending moment of the F-axis is 375.6 KN·m. The maximum axial force of the adjacent column a is 5365 KN. This shows that the horizontal steel truss on the roof forms an alternative load transfer path with the columns above the failure column, and the part of the load above the failure column is transferred to the top steel truss through the columns above, and then is transferred to the adjacent columns. There is also a part of the load that is transferred through the layers of beams to the adjacent columns. In the modified Model 2, the maximum bending moment of the F-axis is 453.4 KN·m. The maximum axial force of the adjacent column a is 5136 KN. The change in the internal force indicates the change in the load transfer path at the lower end of the failure column due to the action of the X-tension reinforcement. In addition, the beam end above the adjacent column a is still a negative bending moment, which increases significantly with the failure of the corner column and is greater than the bending moment of the corresponding beam in Model 1.

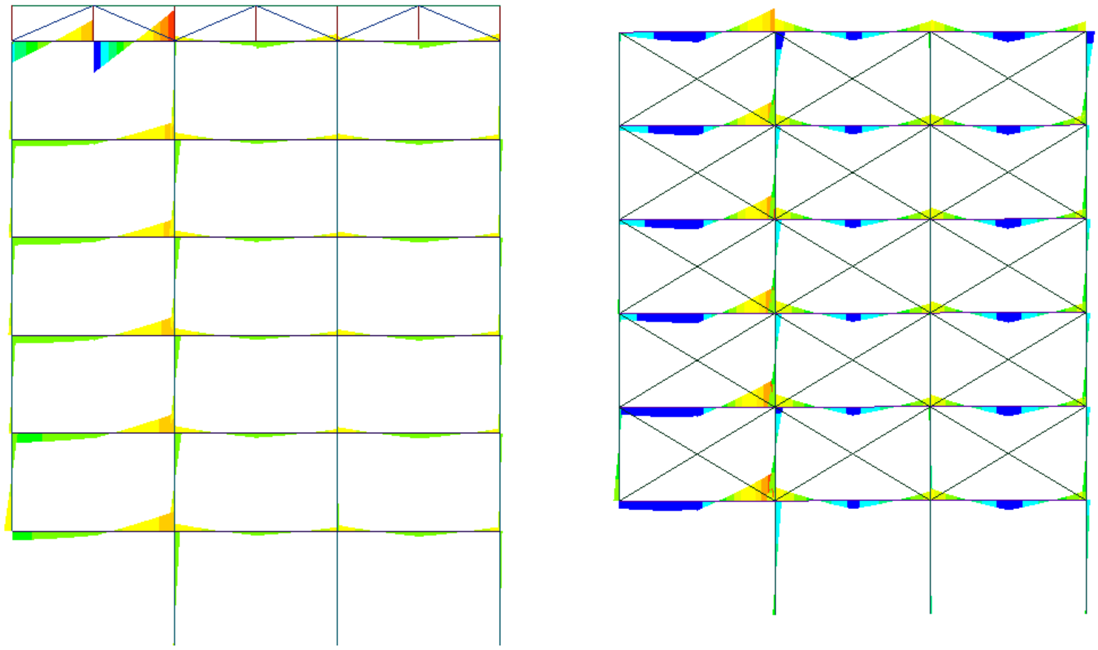

(**a**) (**b**)

Figure 12. The bending moment diagram of F-axis 5 s after column F4 is removed: (**a**) is the bending moment diagram of Model 1; (**b**) is the bending moment diagram of Model 2.

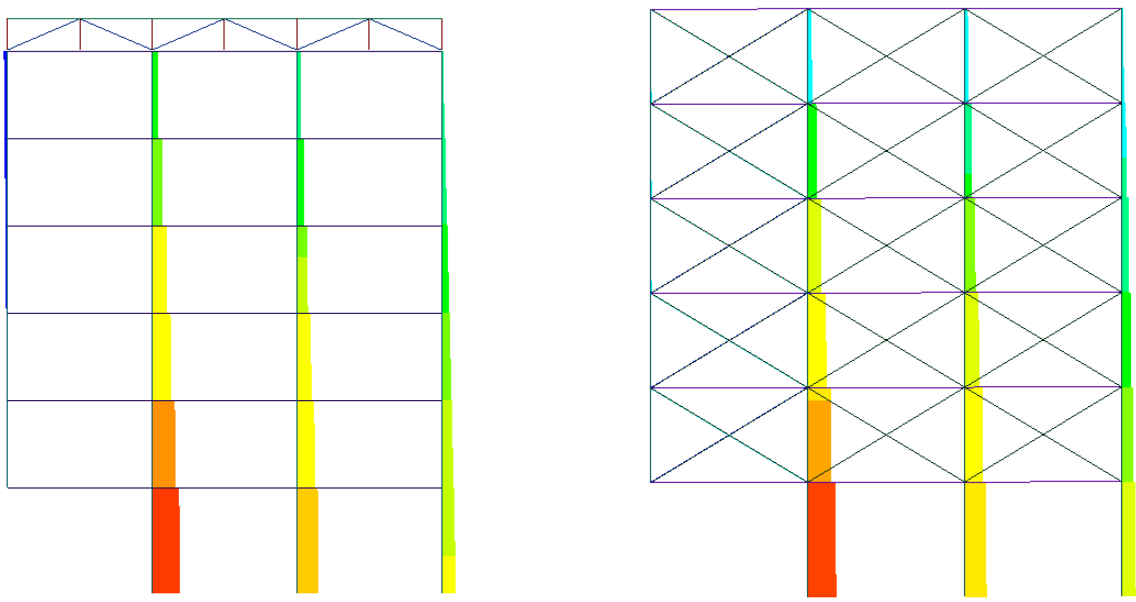

(**a**) (**b**)

Figure 13. Axial force diagram of F-axis 5 s after column F4 is removed: (**a**) is the axial force diagram of Model 1; (**b**) is the axial diagram of Model 2.

By comparing the bending moment diagram and axial force diagram of the two models, it can be seen that the maximum bending moment above the failure column of Model 1 is smaller than that of Model 2. The maximum axial force value of the adjacent columns in Model 1 is greater than that in Model 2. This indicates that the steel truss forms a replacement load transfer path with the columns above the failure column, which can effectively transfer the load above the failure column and distribute it to the adjacent columns. The force transfer effect of the steel truss is better than that of the X tendon.

A comparison of the results of each model when the external convex column of the first layer fails is shown in Table 4.

Table 4. Comparison of the results of each model under working condition 1.

Structure Type	Bending Moment (KN·m)	Column *a* Axial Force (KN)	Vertical Displacement (mm)
Steel roof truss	375.6	5365	53.4
X-tie bar	453.4	5136	76.3
Original structure	513.2	4966	96.6

4.2. The Corner Column at the Concave Corner Is Removed

Figure 14 shows the structure displacement nephogram of Model 1 and Model 2 5 s after removing the D4 column from the first floor. The displacement of each strengthening model is shown in Figure 15. As can be seen from the figure, in the original irregular structure model, the vertical displacement increased significantly before 1.0 s and gradually stabilized to 57.6 mm after 2.4 s. The value is also much smaller than the failure criterion of the progressive collapse of the structure, and thus the structure model does not collapse. In Model 1, when a steel truss was added to the roof, the vertical displacement of the nodes above the failure column increased rapidly before 1.2 s and then fluctuated, and gradually stabilized to 35.6 mm after 4.6 s. Compared with the original structure, the vertical displacement is reduced by 37.8%. With the addition of the X-type tension-strengthening structure in Model 2, the vertical displacement increases rapidly before 0.98 s, and gradually becomes stable at 50.2 mm after 2.3 s. Compared with the original irregular structure, the vertical displacement is reduced by 12.8%.

Compared with the original structure, the vertical displacement of Model 1 is reduced by 37.8%. The vertical displacement of Model 2 is reduced by 12.8%. This shows that both the steel truss and X-type tension reinforcement can form an alternative load transfer path and reduce the vertical displacement of the upper square column caused by the failure of the corner column. However, the effect of the steel truss is more obvious.

Figures 16 and 17 show the bending moment diagram and axial force diagram of the D-axis in the modified Models 1 and 2 when the corner pillar D4 fails for 5 s at the concave corner of the first layer in working condition 2. In Model 1, the maximum bending moment of the D-axis is 335.2 KN·m due to the tensile action of the steel truss in the roof. The maximum axial force of the adjacent column b is 7265 KN. The span of the beam above the failure column is increased two times, and the bending moment of the upper beam end changes from negative to positive, while the far beam end is still negative, and the bending moment of the beams above the failure column increases significantly. This indicates that in Model 1, the adjacent span of the failure column loses the support of the lower column, and the load transfer path changes. The adjacent columns of the failure column and the top steel truss jointly bear the load above the failure column, and a part of the load is transferred from the floor to the secondary beam. It is then transferred from the secondary beam to the main beam, and then distributed to the adjacent columns. A part of the load is transferred through the main beam to the upper square column of the failure column, and then to the top steel truss.

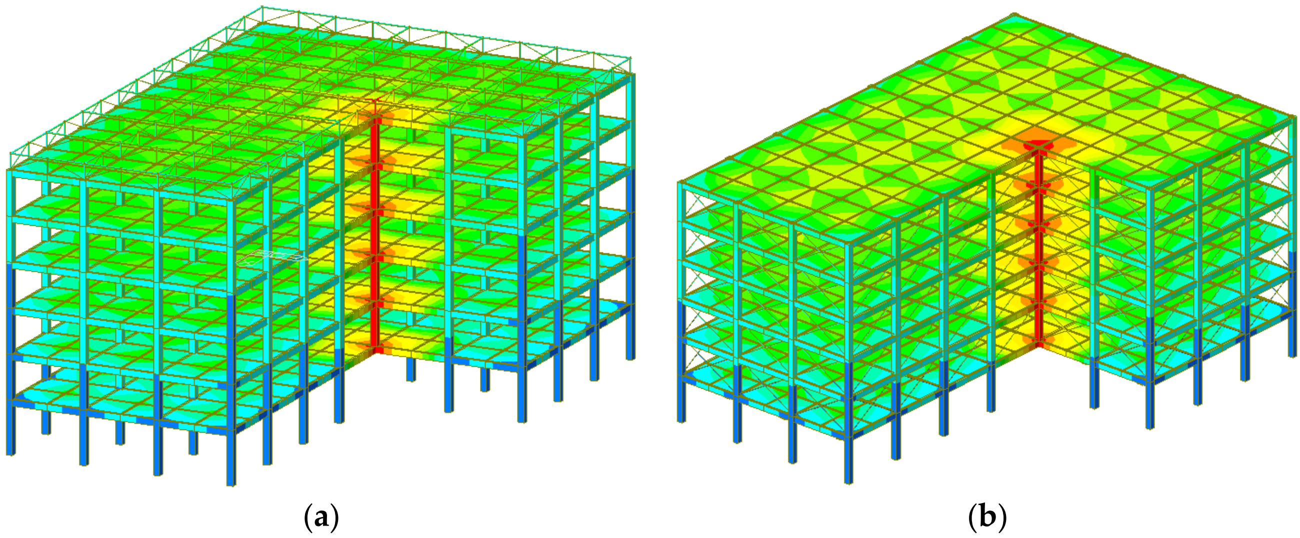

Figure 14. Structural displacement nephogram of column removal at concave corner: (**a**) add steel trusses to the roof of Model 1; (**b**) X-tension reinforcement is added to Model 2 structure.

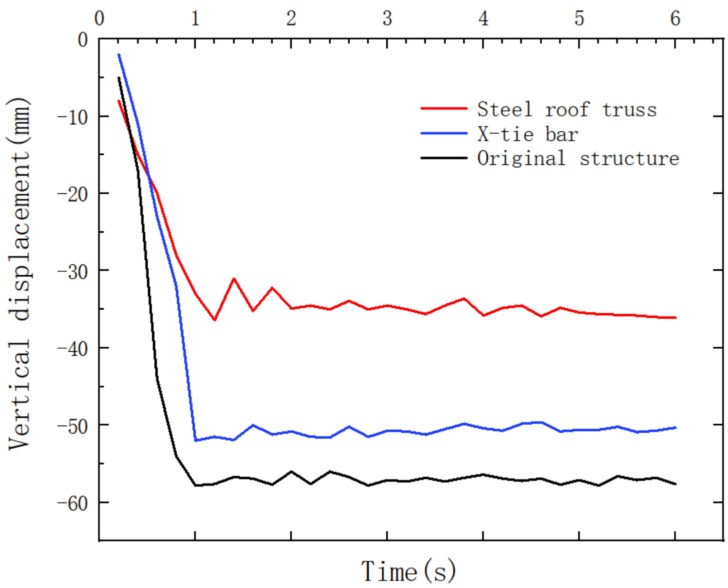

Figure 15. Time-history diagram of removal displacement of corner columns at the concave corners of each model.

In Model 2, the load above the failure column is transferred to the adjacent column mainly through the main beam, and the load transfer process is similar to that in the original model. The axial force of each column above the failure column is small, and the axial compression is the main force being applied. The axial pressure of the adjacent column b increases significantly. The maximum axial force is 7185 KN, but its axial pressure is less than that for the same column in Model 1. The beam ends above the failure column, which is also changed from having negative to positive bending moments, and the maximum bending moment of the D-axis is 461.2 KN larger than that of Model 1. This is because the tying action of the top steel truss in Model 1 shares a part of the load of the beams above the failure column, while in Model 2, there is no top reinforcement and only X-knot bars can be relied on to share the load.

By comparing the bending moment diagram and axial force diagram of the two models, it can be seen that the maximum bending moment above the failure column of Model 1 is smaller than that of Model 2. The maximum axial force value of the adjacent columns in Model 1 is greater than that in Model 2. This shows that the ability of the steel truss to transfer the load above the failure column is better than that of the X-type tension reinforcement.

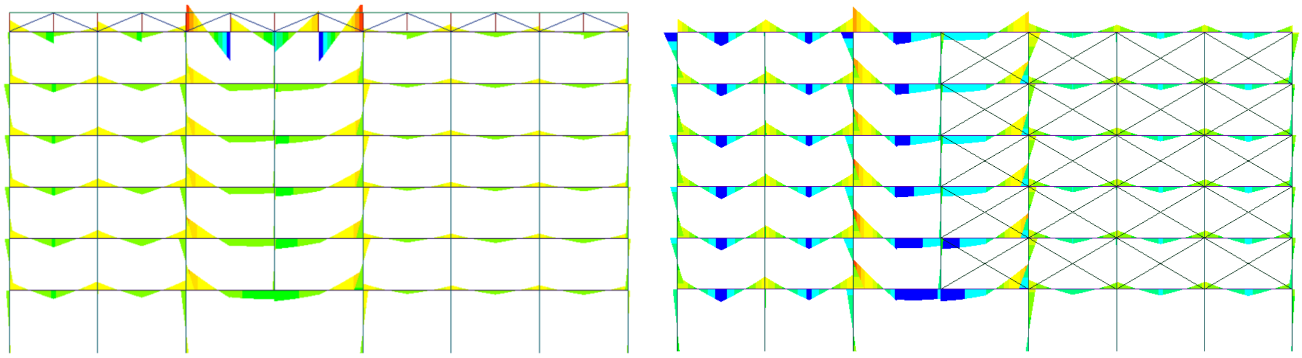

(a) (b)

Figure 16. The bending moment diagram of D-axis 5 s after column D4 is removed: (**a**) is the bending moment diagram of Model 1; (**b**) is the bending moment diagram of Model 2.

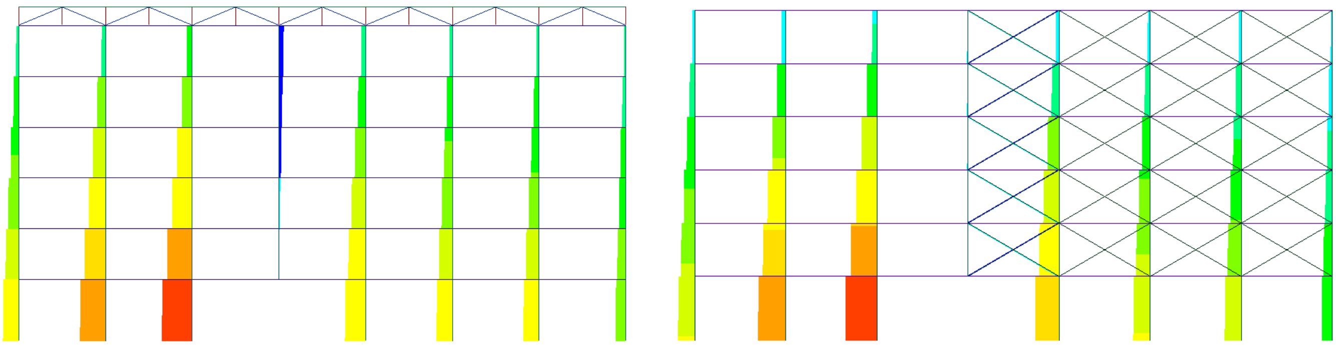

(a) (b)

Figure 17. Axial force diagram of D-axis 5 s after column D4 is removed: (**a**) is the axial force diagram of Model 1; (**b**) is the axial diagram of Model 2.

A comparison of the results of the failure of the column at the concave corner of the first layer of the model is shown in Table 5.

Table 5. Comparison of the results of each model in working condition 2.

Structure Type	Bending Moment (KN·m)	Column *b* Axial Force (KN)	Vertical Displacement (mm)
Steel roof truss	335.2	7265	35.6
X-tie bar	461.2	7185	50.2
Original structure	504.8	6856	57.6

Figure 18 shows the vertical displacement of nodes above the failure column of each model in each working condition. The comparison shows that in Model 1, adding a steel truss to the roof can effectively reduce the vertical displacement of the nodes above the failure column, which is 44.7% and 37.8% of that in the original model. In Model 2, the effect of adding X strengthening to the outside of the structure to reduce the vertical displacement of the nodes above the failure column is not significant, which is 21.1% and 12.8% of that in the original model. In Model 1, adding a steel truss to the roof can reduce the vertical displacement of the nodes above the failure column more effectively. The addition of X-tension strengthening in Model 2 has no significant effect. The effect of adding a steel truss for load transfer above the failure column is more obvious when the corner column of the first floor fails.

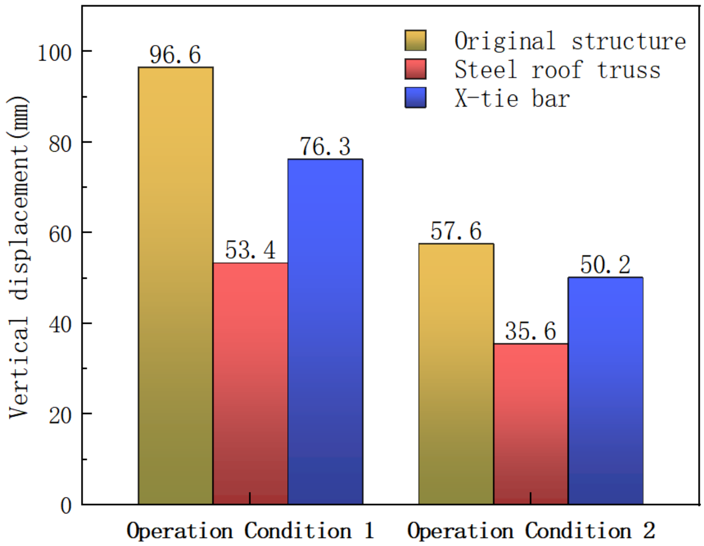

Figure 18. Vertical displacement diagram of nodes above the failure column at 5 s in each working condition of each model.

5. Conclusions

In this paper, the finite element analysis software MIDAS Gen was used for nonlinear dynamic analysis of an L-shaped planar frame structure, and the conclusions are as follows:

(1) In the two cases, the displacement of the node above the original structure failure column was 96.6 mm and 57.6 mm, respectively. This shows that when the angular column fails at the convex part of the first floor, the displacement of the node above the failure column is the largest, which is more likely to cause the progressive collapse of the L-shaped plane frame structure.

(2) When working condition 1 occurs, the far-bending moment of the connecting beam above the failure column of the steel roof truss structure is 375.6 KN·m, and the bending moment value of the structure with the X-tensile reinforcement is 453.4 KN·m. When working condition 2 occurs, the bending moment values are 335.2 KN·m and 461.2 KN·m. The bending moment values of the steel roof truss structures are all smaller than those of structures with X-tensile reinforcement. This shows that the steel truss on the roof forms an alternative load transfer path with the columns of each layer, which can effectively transfer a part of the load above the failure column and provide a larger safety reserve for the structure.

(3) When working condition 1 occurs, the vertical displacement of the failure column of the steel roof truss structure decreases most obviously, decreasing by 44.7%. The vertical displacement of the failure column of the X-tension reinforcement structure is reduced by 21.1%. This indicates that both the steel truss and X-tension strengthening can create a new transmission path for the resistance, and can share a part of the resistance of the beam, transfer the internal force of the failed column to the adjacent column, and improve the anti-collapse ability of the structure. However, the best transmission effect is achieved by adding a steel truss to the roof.

Author Contributions: Conceptualization, methodology and review, Y.D.; numerical models, validation and writing—original draft preparation, L.Q. All authors have read and agreed to the published version of the manuscript.

Funding: This research received no external funding, and the APC was self-funded.

Institutional Review Board Statement: Not applicable.

Informed Consent Statement: Not applicable.

Data Availability Statement: All the analysis data in this paper are from the numerical simulation carried out with finite element software, which was performed to ensure the truth and validity of the data.

Conflicts of Interest: The authors declare no conflict of interest.

References

1. Lin, K.; Chen, Z.; Li, Y.; Lu, X. Uncertainty Analysis on Progressive Collapse of RC Frame Structures under Dynamic Column Removal Scenarios. *J. Build. Eng.* **2022**, *46*, 43–51. [CrossRef]
2. Nyunn, S.; Wang, F.; Yang, J.; Liu, Q.; Azim, I.; Bhatta, S. Numerical Studies on the Progressive Collapse Resistance of Multi-story RC Buildings with and without Exterior Masonry Walls. *Structures* **2020**, *28*, 1050–1059. [CrossRef]
3. Zhang, Q.; Zhao, Y.; Kolozvari, K.; Xu, L. Simplified Model for Assessing Progressive Collapse Resistance of Reinforced Concrete Frames under an Interior Column Loss. *Eng. Struct.* **2020**, *215*, 12–20. [CrossRef]
4. Neeraja, P.; Anish, K. Investigation on progressive collapse failure in a multistorey irregular structure. *Mater. Today Proc.* **2021**, *51*, 538–542. [CrossRef]
5. Esteghamati, M.Z.; Alimohammadi, S. Reliability-based assessment of progressive collapse in horizontally irregular multi-story concrete buildings. *Structures* **2022**, *44*, 1597–1606. [CrossRef]
6. GSA. *Progressive Collapse Analysis and Design Guidelines for New Federal Office Buildings and Major Modernization Projects*; The US General Services Administration: Washington, DC, USA, 2003.
7. Unified Facilities Criteria (UFC)-DoD, Design of Buildings to Resist Progressive Collapse, Department of Defense, USA. 2005. Available online: https://www.wbdg.org/ffc/dod/unified-facilities-criteria-ufc/ufc-4-023-03 (accessed on 10 June 2023).
8. Bandyopadhyay, M.; Banik, A.K. Improvement of progressive collapse resistance potential of semi-rigid jointed steel frames through bracings. *Int. J. Protect Struct.* **2016**, *7*, 518–546. [CrossRef]
9. Yu, J.; Gan, Y.; Ji, J. Behavior and design of reinforced concrete frames retrofitted with steel bracing against progressive collapse. *Struct. Des. Tall Spec. Build.* **2020**, *29*, 102–113. [CrossRef]
10. Ke, C.; Zhang, X. Nonlinear dynamic analysis of the effect of X-type tension reinforcement on RC frame resistance to progressive collapse. *Eng. Seism. Reinf. Modif.* **2022**, *44*, 53–59. (In Chinese)
11. Qiu, L.; Lin, F.; Wu, K. Improving progressive collapse resistance of RC beam-column subassemblages using external steel cables. *J. Perform. Constr. Facil.* **2020**, *34*, 62–75. [CrossRef]
12. Freddi, F.; Ciman, L.; Tondini, N. Retrofit of existing steel structures against progressive collapse through roof-truss. *J. Constr. Steel Res.* **2022**, *188*, 108–116. [CrossRef]
13. Zahrai, S.M.; Ezoddin, A. Cap truss and steel strut to resist progressive collapse in RC frame Structures. *Steel Compos. Struct.* **2018**, *26*, 635–647. [CrossRef]
14. Kiakojouri, F.; Sheidaii, M. Effects of finite element modeling and analysis techniques on response of steel moment-resisting frame in dynamic column removal scenarios. *Asian J. Civil. Eng.* **2018**, *19*, 295–307. [CrossRef]
15. Stephen, D.; Lam, D.; Forth, J.; Ye, J.; Tsavdaridis, K.D. An evaluation of modelling approaches and column removal time on progressive collapse of building. *J. Constr. Steel Res.* **2019**, *153*, 243–253. [CrossRef]
16. Zhao, X.; Shen, B.; Ma, K.; Wang, H.; He, Z.; Zhang, X.; Wu, B. Study on the dynamic analysis method of progressive collapse of plan truss structures. *Prog. Steel Build. Struct.* **2019**, *21*, 15–22. (In Chinese)
17. *UBC-97*; Uniform Building Code; International Conference of Building Official: Washington, DC, USA, 1997; pp. 37–49.
18. *GB 50011-2010*; Ministry of Construction of the People's Republic of China: Code for Seismic Design of Buildings. China Construction Industry Press: Beijing, China, 2010; pp. 58–79. (In Chinese)
19. *GB 50010-2010*; Code for the Design of Concrete Structures. China Construction Industry Press: Beijing, China, 2011; pp. 51–64. (In Chinese)
20. Huang, S.; Guo, X.; Sun, D.; Guan, Y.; Tarasenko, A.A. Shaking table experimental study of damage mechanism of external gallery type RC frame. *Eng. Mech.* **2016**, *33*, 63–71. (In Chinese)
21. Zhang, S.; Cheng, M.; Wang, J.; Wu, J. Modeling the hysteretic responses of RC shear walls under cyclic loading by an energy-based plastic-damage model for concrete. *Int. J. Damage Mech.* **2020**, *29*, 107–124. [CrossRef]
22. Jiao, Y.; Wang, B.; Shen, Z. A New 3D Empirical Plastic and Damage Model for Simulating the Failure of Concrete Structure. *Int. J. Concr. Struct. Mater.* **2019**, *13*, 118–137. [CrossRef]
23. Li, Z. Research on Progressive Collapse Resistance of Structure Based on Alternative Path Method. Ph.D. Thesis, Tianjin University, Tianjin, China, 2013. (In Chinese).
24. Guo, J. Numerical Analysis of Influence of Cast-in-Place RC Floor on Progressive Collapse Resistance of Frame. Master's Thesis, Chang'an University, Xi'an, China, 2019. (In Chinese).